
REAL-TIME AERIAL DETECTION AND REASONING ON EMBEDDED-UAVS IN RURAL ENVIRONMENTS

Tin Lai[†]

oscar@tinyiu.com
School of Computer Science
University of Sydney
Australia

ABSTRACT

We present a unified pipeline architecture for a real-time detection system on an embedded system for UAVs. Neural architectures have been the industry standard for computer vision. However, most existing works focus solely on concatenating deeper layers to achieve higher accuracy with run-time performance as the trade-off. This pipeline of networks can exploit the domain-specific knowledge on aerial pedestrian detection and activity recognition for the emerging UAV applications of autonomous surveying and activity reporting. In particular, our pipeline architectures operate in a time-sensitive manner, have high accuracy in detecting pedestrians from various aerial orientations, use a novel attention map for multi-activities recognition, and jointly refine its detection with temporal information. Numerically, we demonstrate our model's accuracy and fast inference speed on embedded systems. We empirically deployed our prototype hardware with full live feeds in a real-world open-field environment.

1 Introduction

Real-time awareness and understanding of the physical world have long been open questions for the robotics community. For machines to successfully manoeuvre in the presence of dynamic obstacles, e.g. autonomous car driving within a crowd, one must perceive the intention of the humans and respond appropriately. A real-time anomaly monitor system is crucial for crowd monitoring during mega-events (Schulte, Hillen and Prinz 2017), where the system must recognise any hostile intentions that any individuals might be planning to perform. Moreover, an autonomous aerial surveying system in a search and rescue mission (Abdelkader, Shaqura, Claudel et al. 2013) will require the ability to comprehend the state of any detected humans and reports accordingly (Hildmann and Kovacs 2019); significantly when the number of dispatched drones greatly exceed the number of human operators (Aljehani and Inoue 2016).

All the mentioned applications have a common interest—the ability to perform semantic understanding directly on a remote machine. While some applications could be achieved with a centralised approach, i.e. perform semantic inferences on a centralised server farm, most existing infrastructure will have difficulties implementing such an approach. For example, wireless bandwidth will be restricted for transferring video footage to a remote server from drones (Merino, Caballero, Martínez-de Dios et al. 2006; Sahingoz 2013; Vega, Lin, Swaminathan et al. 2015). This is especially true during a search and rescue operation, where internet access might be unavailable, or the bandwidth is limited to reserve for critical communication. Moreover, some privacy-sensitive applications might want to avoid sending sensitive information over the air to a server (K. Huang, Ximeng Liu, S. Fu et al. 2019). Therefore, for specific applications, directly performing inferences on the embedded system of the remote hardware is the only approach.

The scope of this paper is on performing decentralised real-time autonomous activity reporting in a remote area, focusing on semantic understanding of people's current status from Unmanned Aerial Vehicles (UAVs) perspective. UAVs play a crucial role when operating in rural environments, for tasks such as disaster response and recovery

[†]Part of the work was done while Tin Lai was visiting the National Institute of Informatics, Tokyo 101-8430, Japan.



Figure 1: Deploying live detection and recognition in the field of *Okutama, Japan* (top). Spatial locations of detected pedestrians, recognised actions and confidence scores are all processed on-board directly for transmitting to remote server. The processed information is overlaid on original video images for visualisation (bottom).

operations, where ground access is infeasible in the aftermath of natural disasters such as earthquakes. It has been commonplace for mayors and governments to pursue mega-events to develop or regenerate their cities. Mega-events, such as festive carnival, can bring positive socio-economic benefits to the city. However, mega-events bring substantial strains to the security or police forces to monitor the environment, especially when human resources are scarce. Similarly, in disastrous situations, autonomous UAVs surveying is hugely desirable due to the area of land they can cover. Victims can be located faster and reached earlier when UAVs are deployed in mountain search and rescue operations (Karaca, Cicek, Tatli et al. 2018). However, current approaches transfer multi-gigabytes of video footage from remote drones to a centralised server for analysis. Network activities are severely limited in disaster area (Y. M. Chen, Dong and J.-S. Oh 2007), and any wireless bandwidth should be preserved for the communication channel between emergency services (Bai, Du, Ma et al. 2010) and critical communication. Therefore, it severely limits relying on centralised servers for video processing.

On the other hand, lightweight models such as MobileNetV2 (Sandler, Howard, Zhu et al. 2018) can achieve reasonable runtime speed but sacrifices predictive performance on aerial-captured images due to the highly varying camera angles from UAVs' perspective. Although they are suitable for static embedded systems, the severely limited inference quality poses difficulty for usage on UAVs. To this end, we propose our framework with the following properties. We will employ UAVs with an embedded camera on board to survey an area of interest and report any abnormality to operators—namely, the current status of the detected pedestrians and associated GPS coordinates. The problem setup requires a sizeable amount of inexpensive UAVs patrolling the vast aerial space for search and rescue; therefore, each UAV must operate autonomously and raise alerts if necessary. Each UAV will be equipped with an embedded system and a pre-trained model for surveying.

This paper proposes a lightweight model pipeline that simultaneously detects pedestrians and recognises their current status. Furthermore, our model is lightweight with minimal parameters and suitable for real-time processing in an onboard system. A novel regression-based approach first performs preliminary human detection to address the camera perspective variance issue. Then, the preliminary results are further refined by information from the framework’s temporal layers to jointly recognise the detected pedestrians’ current status. Therefore, it uses minimal resources to detect abnormality directly on remote drones. We deployed the live system at a remote field with real-time tracking and status reports delivered to the user through wireless transmission (Fig. 1) and provided comprehensive numerical results on the model performance.

2 Related works

Recent advancements in deep learning provide a robust framework for developing applications for vision-based problems. In contrast to traditional computer vision techniques with handcrafted features, deep neural networks can learn features directly from training data as a data-driven approach, achieving superior results than previous approaches.

2.1 Pedestrian Detection

Recent works on convolutional and recurrent neural networks enable deformation and occlusion handling (Ouyang and Xiaogang Wang 2013), using Convolutional Neural Network (CNN) to detect objects of interest from UAVs imagery (Bejiga, Zeggada, Nouffidj et al. 2017), and using multiple part detectors to combine as a pedestrian detector (Tian, Luo, Xiaogang Wang et al. 2015). Object detections mainly utilise a sliding window approach or object proposal mechanism (Ren, He, Girshick et al. 2015). Deep learning had tremendous successes in suppressing traditional feature-extraction methods in many other fields, for example, in natural science (Xiaoting Xu, Lai, Jahan et al. 2022), medical science (Hu, Lai and Farid 2022), or even in financial sectors (Xipei Wang, H. Zhang, Y. Zhang et al. 2022). These methods demonstrated the representation power of deep learning on complicated problems, which are often hard to accomplish with handcrafted features. However, they do not jointly reason the detected object with their temporal information, relying only on convolutional layers. Recent works have framed object detection as a regression problem (Redmon, Divvala, Girshick et al. 2016) by densely generating bounding boxes with spatial separation afterwards.

Robust human detection is an essential part of the UAV system as it facilitates capturing the locations of humans and reasoning on their current actions. UAV imagery in object detections (Xiaoliang Wang, Cheng, Xinchuan Liu et al. 2018; R. Zhang, Shao, X. Huang et al. 2020; Kraft, Piechocki, Ptak et al. 2021) had been a specific subfield in computer vision. Video feeds captured on UAVs are usually overhead shots with a wide variety of orientations, often highly varying compared to typical person detection (Häger, Bhat, Danelljan et al. 2016; Dike, Wu, Zhou et al. 2018; Sambolek and Ivacic-Kos 2020).

2.2 Activities Understanding

Action understanding helps provide context on the detected person’s current activities. It is also a crucial aspect of a disaster response system as it provides contextual and situational information for the captured scenes (J. Yang, Xie and Wenzhe Yang 2019). Most current approaches to multi-pedestrian action recognition take a sequential approach by

Algorithm 1: Overall model description

```

1 while Not terminated do
2    $\mathcal{I}_t \leftarrow$  fetch latest image from camera at  $t$ 
3    $\mathcal{F}_t \leftarrow$  extract multiscale dense features from  $\mathcal{I}_t$ 
4    $\mathcal{S}_t, \mathcal{R}_t \leftarrow$  outputs from two separated convolutional layers with  $\mathcal{F}_t$  as input
5    $\hat{\mathbf{b}}_t \leftarrow$  BoxGenerator( $\mathcal{S}_t, \mathcal{R}_t$ ) ▷ Alg.2
6    $\hat{\mathbf{f}}_t \leftarrow$  crop  $\mathcal{F}_t$  with each  $b_t \in \hat{\mathbf{b}}_t$ 
7   associate each  $f_t \in \hat{\mathbf{f}}_t$  with the corresponding  $f_{t-1} \in \hat{\mathbf{f}}_{t-1}$  from previous time step
8   generate  $A_{t,i}$  and concat to each  $f_t \in \hat{\mathbf{f}}_t$  ▷ Eq.5
9    $\hat{\mathbf{a}}_t, \hat{\mathbf{c}}_t \leftarrow$  predict actions and confidence scores from the recurrent neural network with input  $\hat{\mathbf{f}}_t | \hat{\mathbf{f}}_{t-1}$ 
10  use  $\hat{\mathbf{c}}_t$  with non-maximum suppression on  $\hat{\mathbf{b}}_t$  and  $\hat{\mathbf{a}}_t$ 
11  output  $\hat{\mathbf{b}}_t, \hat{\mathbf{a}}_t, \hat{\mathbf{c}}_t$  to user
    
```

separating each component and optimising each part separately. Human is first detected in a CNN model and tracked with an algorithm, then feature representations are extracted for each person to reason on their action (Ramanathan, J. Huang, Abu-El-Haija et al. 2016). This approach requires much processing time as it needs to repeat the process for each detected person, which does not scale well on a UAV system. A 3D CNN has also been proposed for action recognition (Ji, W. Xu, M. Yang et al. 2013), which is based on a similar concept to regular CNNs with extra convolutions in the temporal axis. Such an approach can often achieve high accuracy with the expenses of computational overhead (Sozykin, Protasov, Khan et al. 2018; H. Xu, Das and Saenko 2017), often a limiting factor in UAV systems. It achieves high accuracy in action understanding with the cost of substantial computational time. Therefore, the limitation of computational power and batteries on modern UAVs restrict the technique’s applicability to perform inferences directly onboard.

2.3 Attentive Mechanism

Recent works on the visual attention model gained a lot of empirical achievements, which is particularly important for interpreting the recognition of objects in cluttered scenes (Borji and Itti 2012). They act as a selection mechanism that encodes the notion of relevance regarding the overall rich stream of visual data. Visual attention can guide the computational models, such as a neural network, to essential parts of the scene to gather more local information (H. Zheng, J. Fu, Mei et al. 2017). Attention map has been proven to be an effective way to allow neural nets to focus on local details that are more semantically important for enhancing overall results. For example, (Hong, J. Oh, Lee et al. 2016) uses semantic segmentation as an attention map to transfer knowledge across the domain. A context-attention map generated with another neural net can be utilised to improve human pose estimation (Chu, Wei Yang, Ouyang et al. 2017). Gaussian Mixture Attention Maps have also previously been used as a depth feature to learn and reason jointly on multiple channels jointly (C. Wang and Siddiqi 2016). However, most approaches require a separate neural network to generate an additional attention layer, which is computationally prohibited on embedded systems with limited hardware.

We propose a simple yet effective way to produce a pseudo-attention map for our bounding box expansion. Empirically, we show that expanding the bounding box helps improve the accuracy of temporal reasoning. Furthermore, the added attention map layer further improves the result by encoding the semantic spatial information to the expanded boxes.

2.4 Embedded Systems in UAVs

Most meaningful tasks for autonomous operations of UAVs require a combination of advanced sensors, complex image processing procedures and flight control algorithms (Al-Kaff, Martin, Garcia et al. 2018). Traditional algorithms and models that perform well in a ground station might not be suitable in the embedded system in UAVs. For example, (Hulens, Goedemé and Verbeke 2015) discussed the trade-off between speed, power consumption and the weight of specific hardware platforms when operating in UAVs. Advanced and computationally expensive algorithms are not directly applicable to operation on embedded devices. Autonomous operations of drones require substantial computational resources on tasks such as SLAM (Lai 2022) for localisation, motion planning (Lai and Ramos 2022) of aircraft for planning trajectories, often in the kinodynamic space (Lai, Zhi, Hermans et al. 2022) for acceleration controls. Therefore, using minimal computational resources on computer vision models is essential for the real-time operation of autonomous UAVs. However, this approach uses numerical and graphical indicators to assess the vegetation properties instead of a deep-learning approach to maintain low computational overhead. Successful usage of vision-based approaches in UAVs includes applications such as Friesian cattle recovery (Andrew, Greatwood and Burghardt 2019), counting vehicles in traffic (Amato, Ciampi, Falchi et al. 2019), and drone safe landing (Kakaletsis, Symeonidis, Tzelepi et al. 2021). The computational power and sensor requirements for UAVs’ computer vision tasks are often different than that of an offline counterpart (Douklias, Karagiannidis, Misichroni et al. 2022). Therefore, it is necessary to consider the physical hardware limitations when designing UAVs’ computer vision applications.

3 Methodology

We propose a unified architecture for a real-time system deployed in UAVs for autonomous surveying. To this end, we designed our model to be lightweight and memory-efficient for usage on an embedded system. We propose a detection network specifically for detecting pedestrians captured in different orientations and combined with a temporal network for jointly recognising individual activities.

3.1 Overview

The overview of our entire architecture is shown in Fig. 2, and overall description is given in Alg. 1. Our architecture is composed of a pedestrian detection model, specifically designed for aerial surveying, as the entry point of the

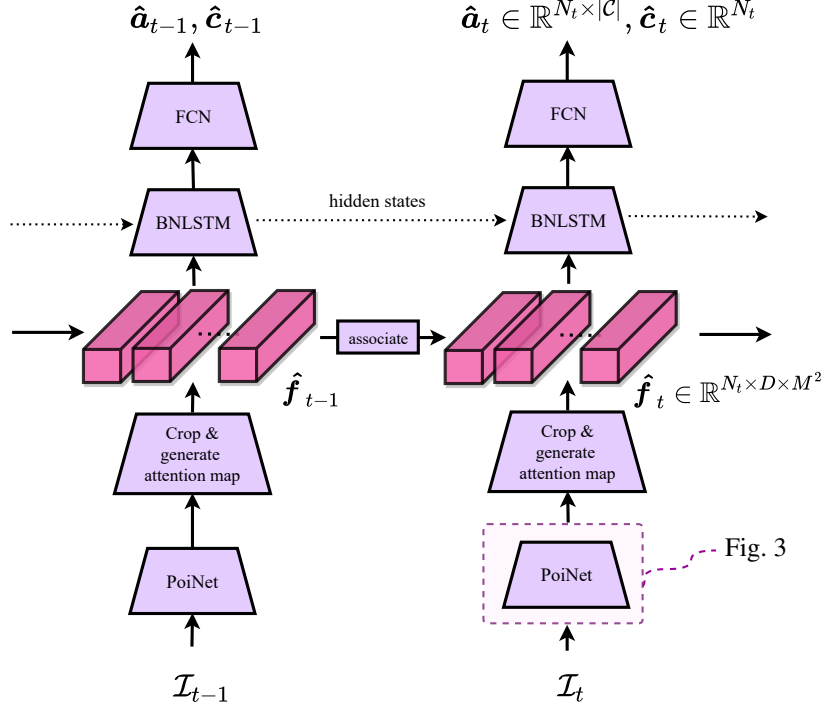


Figure 2: Overview of our entire framework. Frame \mathcal{I}_t are queried at each time-step t and passed through our POINet (Fig. 3) to generate bounding boxes \hat{b}_t on the given frame, which is then used to crop on the original dense feature map to extract fixed-size \hat{f}_t . The extracted dense features are first concatenated with the generated attention map, then passed to a BNLSTM to reason on the temporal information. The final outputs are the probability of each recognised activity \hat{a}_t and confidence scores \hat{c}_t to suppress low confidence bounding box.

architecture. Each video frame at time t , which we denoted with \mathcal{I}_t , is input into the detection network (section 3.2). The output is a dense multiscale feature \mathcal{F}_t , of which we will extract the bounding boxes into a fixed size $\hat{f}_t \in \mathbb{R}^{N_t \times D \times M^2}$ representation. The following components further extract temporal information from the dense features, which will be referred to as *ActivityNet* (section 3.3). Finally, the model outputs multiple bounding boxes on pedestrians detection with associated multidimensional predicted actions and confidence scores.

3.2 POINet

This section will formulate the pipeline and architecture of our Position and Orientation Invariant detection Network (POINet) model. This model is responsible for producing bounding boxes of any detected pedestrian in our framework. The challenge lies in the UAVs' operating camera angles, which often vary significantly due to the problem setup's nature. We incorporated traditional computer vision in the generation of bounding boxes. The use of fast and robust computer vision techniques is combined with the extracted features from CNN for its representation power. Therefore, our approach uses less computational resources and time compared to approaches that use dense proposals of bounding boxes (Redmon, Divvala, Girshick et al. 2016). An example of typical UAV imagery is shown in Fig. 4e, where the size of pedestrians (and bounding boxes) are incredibly tiny compared to the overall frame size. Furthermore, in aerial surveying, most video feeds are recorded in many different possible orientations, which creates severe challenges to robust detection. For example, Fig. 5c illustrates several examples of pedestrians captured in bird's-eye shots, high-angle shots, and near side-view shots. POINet addresses these issues by first extracting multiscale features, then using segmentation and regression maps for anchoring the location of each detected pedestrian.

3.2.1 Anchoring Bounding Boxes

The extracted frame \mathcal{I}_t from the input video feed is first fed into some lightweight CNN to extract high dimensional features. To this end, we used MobileNetV2 for feature extractions aimed at embedded hardware by design (Sandler, Howard, Zhu et al. 2018). During aerial surveying, pedestrians are often captured at different scales with no fixed

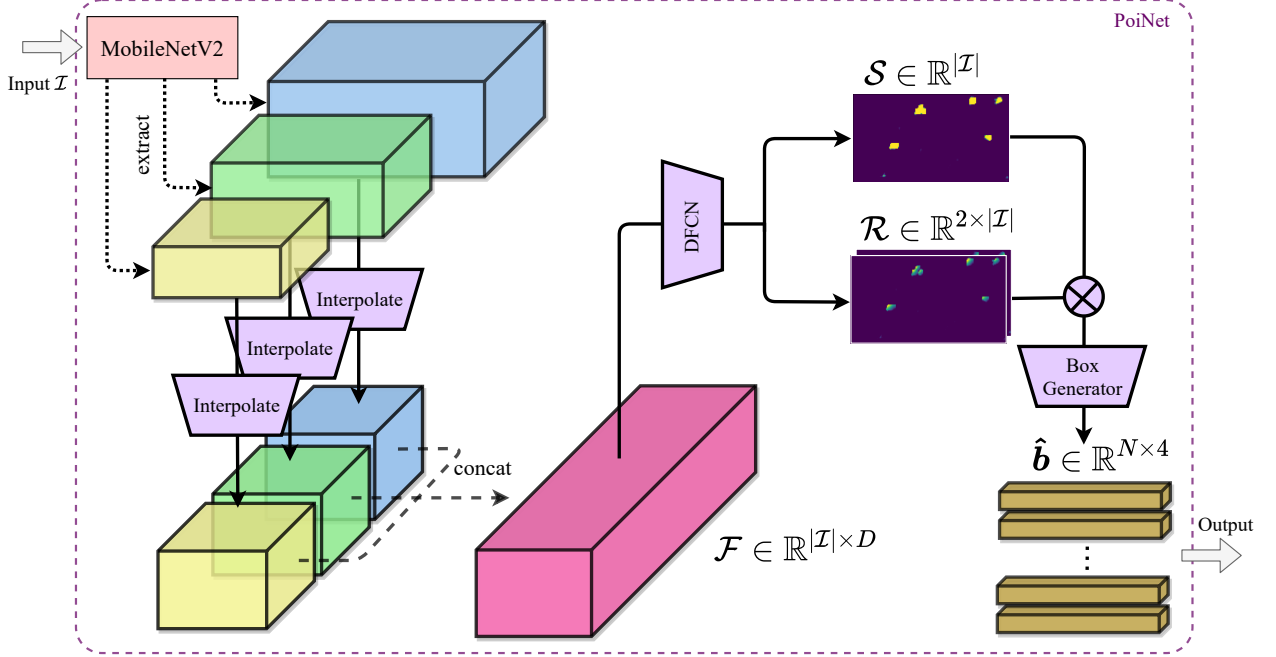


Figure 3: Overview of the POINet architecture, detailing the transformations of the input image data for robust pedestrians detection.

zoom level. Therefore, we extract high-dimensional features at different scales and then further concatenate them as multi-scale dense features \mathcal{F}_t . With the extracted \mathcal{F}_t , POINet uses basic convolutional layers to generate segmentation map $\mathcal{S} \in \mathbb{R}^{|\mathcal{I}|}$ and regression maps $\mathcal{R} \in \mathbb{R}^{2 \times |\mathcal{I}|}$. Semantically, the segmentation map \mathcal{S} represents the area of interest that the POINet is trained on; whereas the regression map \mathcal{R} contains the spatial information of the bounding boxes. Segmentation map \mathcal{S} and regression maps \mathcal{R} are each given a ground truth that consists of crucial spatial information to reconstruct bounding boxes (Bagautdinov, Alahi, Fleuret et al. 2017).

We convert the ground truth pedestrian location into dense maps \mathcal{S} and \mathcal{R} with the following. For each captured image \mathcal{I}_t at time t , the ground truth consists of a set of bounding boxes $\hat{\mathbf{b}} \in \mathbb{R}^{N_t \times 4}$ where $b_i \in \hat{\mathbf{b}}$ consists of the location information $(x_0, y_0, x_1, y_1)_t$ and N_t is the number of groundtruth boxes for \mathcal{I}_t . The \mathcal{S} and \mathcal{R} are defined over all the specific location $\mathbf{i} = (i_x, i_y) \in \mathcal{I}$, where we will use $\mathcal{S}_i, \mathcal{R}_i$ to denote their values at (i_x, i_y) . For the segmentation map \mathcal{S} , we define

$$\mathcal{S}_i = \begin{cases} 1 & \text{if } x_0 \leq i_x \leq x_1 \wedge y_0 \leq i_y \leq y_1 \\ 0 & \text{otherwise,} \end{cases} \quad (1)$$

such that it overlays areas with pedestrians. Fig. 4a demonstrates an example of a segmentation map \mathcal{S} , which allows the model to learn the semantic patterns of pedestrians. For the regression map \mathcal{R} , each location (i_x, i_y) is a vector $\mathcal{R}_i = [r_0 \ r_1]^\top$ that encodes the spatial location—top-left and bottom-right diagonal corners—of the bounding box, respectively. We define $\mathcal{R}_i = [0 \ 0]^\top$ if $\mathcal{S}_i = 0$. For pixels i within the segmented area (i.e. $\mathcal{S}_i = 1$), we define \mathcal{R}_i to be in the range of 0 to 1, such that

$$\mathcal{R}_i = \begin{bmatrix} r_0 \\ r_1 \end{bmatrix} = \frac{1}{\alpha} \begin{bmatrix} x_1 - i_x & y_1 - i_y \\ i_x - x_0 & i_y - y_0 \end{bmatrix} \begin{bmatrix} \cos \theta \\ \sin \theta \end{bmatrix} \quad (2)$$

where

$$\theta = \arctan(y_1 - y_0) / (x_1 - x_0) \quad (3)$$

is the angle of the diagonal and

$$\alpha = \sqrt{(y_1 - y_0)^2 + (x_1 - x_0)^2} \quad (4)$$

is the normalising constant. Figs. 4b and 4c illustrate an example of the regression maps \mathcal{R} which allow the model to spatially learn the anchor points for the bounding boxes of pedestrians.

During inference, we begin by first extracting the area of interest by obtaining \mathcal{R}' in Alg. 2 line 2. We will then remove noises in \mathcal{R}' that only contain a tiny contiguous area of patches. Afterwards, we apply a maximum filter across \mathcal{R}'

Algorithm 2: Bounding box generator

Parameter δ : minimum percentage of segmented area

```

1 function BoxGenerator( $S, \mathcal{R}$ )
2    $\mathcal{R}' \leftarrow S \cdot \mathcal{R}$   $\triangleright$  extracts area of interest
3   remove noise (tiny area of patches) in  $\mathcal{R}'$ 
4    $\hat{p} \leftarrow$  find local maxima in  $\mathcal{R}'$  via maximum filter
5    $\triangleright$  now  $\hat{p}_1$  contains the top left and  $\hat{p}_2$  contains the bottom right coordinates of the candidate boxes
6    $\hat{b} \leftarrow$  combinations of  $\hat{p}_1$  and  $\hat{p}_2$ 
7    $\triangleright \hat{b}$  is a set of box corner coordinates
8    $\hat{b}' \leftarrow \emptyset$ 
9   foreach  $b \in \hat{b}$  do
10     $B \leftarrow$  set of pixels enclosed by the box  $b$ 
11     $B' \leftarrow \left\{ i \in B \mid \begin{array}{l} i \text{ is segmented as pixels} \\ \text{of interest in } S \end{array} \right\}$ 
12    if  $|B'| / |B| \geq \delta$  then
13       $\hat{b}' \leftarrow \{b\} \cup \hat{b}'$ 
14  return  $\hat{b}'$   $\triangleright$  set of bounding boxes
    
```

(Figs. 4b and 4c) to obtain box corner coordinates, which are then used to densely generate multiple bounding boxes \hat{b} . Finally, we programmatically remove boxes that contain less than $\delta \in \mathbb{R}, 0 < \delta \leq 1$ fraction amount of segmented pixels (lines 8 to 11), and practically we set $\delta = 0.9$.

3.2.2 Incorporating Temporal Information in Pedestrian Detection

While spatial information is crucial for pedestrian detection, temporary changes can often negatively influence the detection accuracy due to changes in perspective or occlusion (Xiaoyu Wang, Han and Yan 2009). Therefore, POINet is designed to densely generate bounding boxes and then jointly refined by the leaked temporal information from the activity layers. *ActivityNet* (section 3.3) is located at the end of our pipeline (Fig. 2), which uses temporal information to predict the current activity of each detected pedestrian and associated confidence scores $\hat{c}_t \in \mathbb{R}^{N_t}$. The confidence scores are then used to jointly refine the bounding boxes $\hat{b} \in \mathbb{R}^{N_t \times 4}$ with non-maximum suppression (Neubeck and Van Gool 2006). Non-maximum suppression is a technique to select one entity out of many overlapping entities based on the boxes' probability and the measure of the overlapping region with the Intersection over Union (IoU) metric. We can choose the selection criteria to arrive at the desired results. The leaked confidence scores from the activity component are used to help jointly enhance the refinement of the bounding box proposer.

3.3 ActivityNet

The activity detection component of our *ActivityNet* framework takes input directly from POINet to learn temporal information. With each detected pedestrian, a novel attention map-based approach is first used to improve the effectiveness of learning activities (section 3.3.1). Afterwards, we pass the cropped dense pedestrian features to a Batch Normalised Long Short-Term Memory (BNLSTM) block (Cooijmans, Ballas, Laurent et al. 2017) as detailed in section 3.3.2.

3.3.1 Attention map

We employ a novel attention map-based technique (H. Zheng, J. Fu, Mei et al. 2017) to facilitate adding additional contextual information to each bounding box. It enables a programmatic way to incorporate the bounding boxes' surrounding environment while maintaining the spatial information of the boxes. With the approach in (Bagautdinov, Alahi, Fleuret et al. 2017) of directly using the cropped boxes as the input features, the boxes will lose much contextual information in the background—which is arguably essential for learning the activities. Here we are employing a simple yet effective approach to incorporate more contextual information and the bounding box. In addition, the attention map approach also allows us to avoid introducing distortion of aspect ratio for the cropped images, which is common in many RNN approaches. However, previous studies found that distorted aspect ratio region tends to give higher false-positive bounding boxes (Z. Xu, Xin Xu, L. Wang et al. 2017), where preserving the shape of objects is highly beneficial for accurate classification (L. Zheng, Zhao, S. Wang et al. 2016).

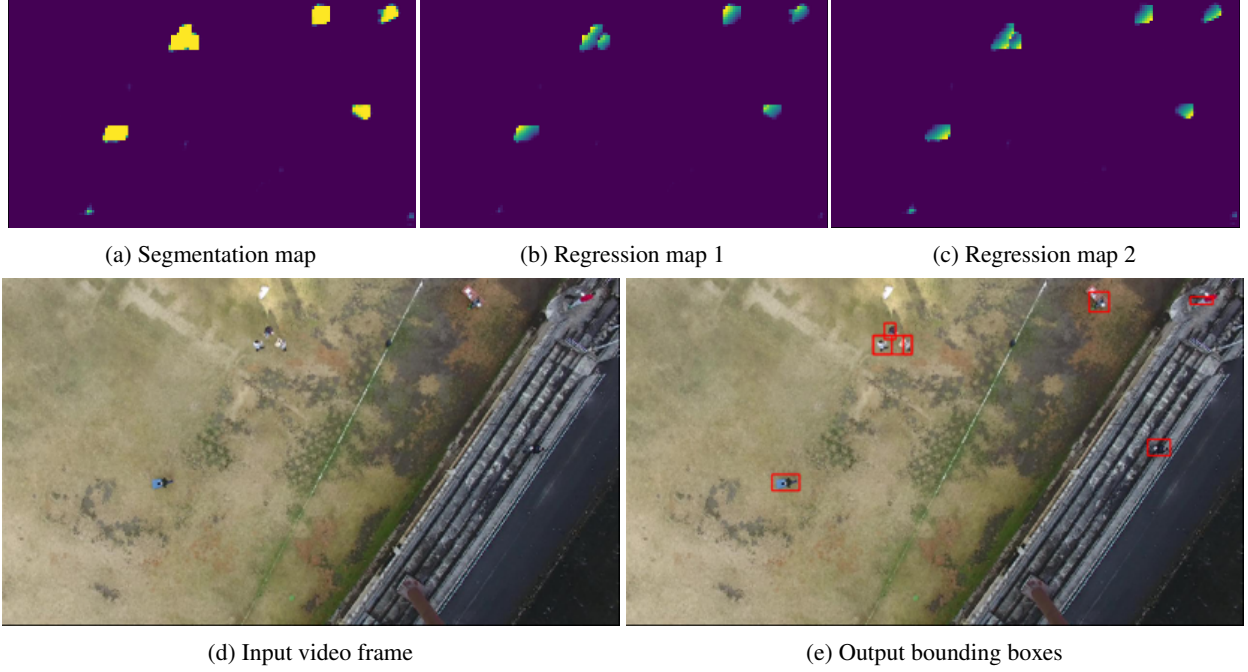


Figure 4: Generating bounding boxes by extracting spatial information from the images. (d) Captured video frames are first feed into POINet. The network will outputs (a) segmentation map and (b, c) regression maps of which summarised the points of interest that the POINet is trained on. The maps will then be passed to several filters and suppression algorithms to output (e) final bounding boxes.

The attention matrix A uses a flexible multivariate Gaussian kernel to encode the likely correlation of the expanded region of the bounding box while allowing our temporal network to reason on previously absent contextual information. We define the attention matrix as $A \in \mathbb{R}^{M \times M}$ where $M = \lceil \alpha \cdot \max(W, H) \rceil$ is the dimension of the expanded bounding box, and $\alpha \in \mathbb{R}, \alpha \geq 1$ is a factor that controls the ratio of expansion. The values of the attention matrix are defined as

$$A_i = \begin{cases} 1 & \text{if } x_0 \leq i_x \leq x_1 \wedge y_0 \leq i_y \leq y_1 \\ \varphi(i | \mathbf{b}_e, \Sigma) & \text{otherwise,} \end{cases} \quad (5)$$

where $\varphi(\mathbf{x} | \boldsymbol{\mu}, \Sigma) = \exp\{-\frac{1}{2}(\mathbf{x} - \boldsymbol{\mu})\Sigma^{-1}(\mathbf{x} - \boldsymbol{\mu})\}$ resembles the probability density distribution of the multivariate Gaussian (Bishop 2006) without normalising factor, Moreover, Σ is a positive definite covariance matrix that encodes our belief on the spatial correlation between the action of the pedestrians and their surrounding environment. Section 4 provides experimental results on the effectiveness of the additional attention map. The flexibility of this novel attention map allows us to express the relevance of each pixel to the surrounding contextual information. We formulate an algorithmic way to generate a pseudo-attention map based purely on the given bounding box ground truth. In addition, this novel method directly avoids distortion of cropped images, and experimentally, we show that the additions of the attention map enhance the overall model accuracy.

3.3.2 Training POINet and ActivityNet End-to-End

We have described a way to obtain a set of reliable detection from raw images from previous sections. However, temporal information was shown to be important in action recognition and provide a valuable basis for reasoning on detection. Therefore, after obtaining predictions by the BNLSTM component in Fig. 2 we utilise the temporal confidence score \hat{c}_t by jointly refining the detected bounding boxes. That is, we use confidence scores to refine and suppress low confidence bounding box with non-maximum suppression (Neubeck and Van Gool 2006). The reason is that temporal information can often provide a better estimate of whether the captured bounding box contains a pedestrian.

For each frame \mathcal{I}_t , given that we had extracted N bounding boxes of pedestrian $\hat{\mathbf{b}}_t = \{\mathbf{b}_t^1, \dots, \mathbf{b}_t^N\}$, we extract a fixed-sized representation $\hat{\mathbf{f}}_t = \{f_t^1, \dots, f_t^N\}$ for each box from the multiscale dense feature \mathcal{F}_t . These embeddings are then sent to our BNLSTM block, which produces predictions on their corresponding activities $\hat{\mathbf{a}}_t$ and confidence scores \hat{c}_t that denote the likelihood that the sequence of frames contains actual pedestrians. Finally, we construct a loss that

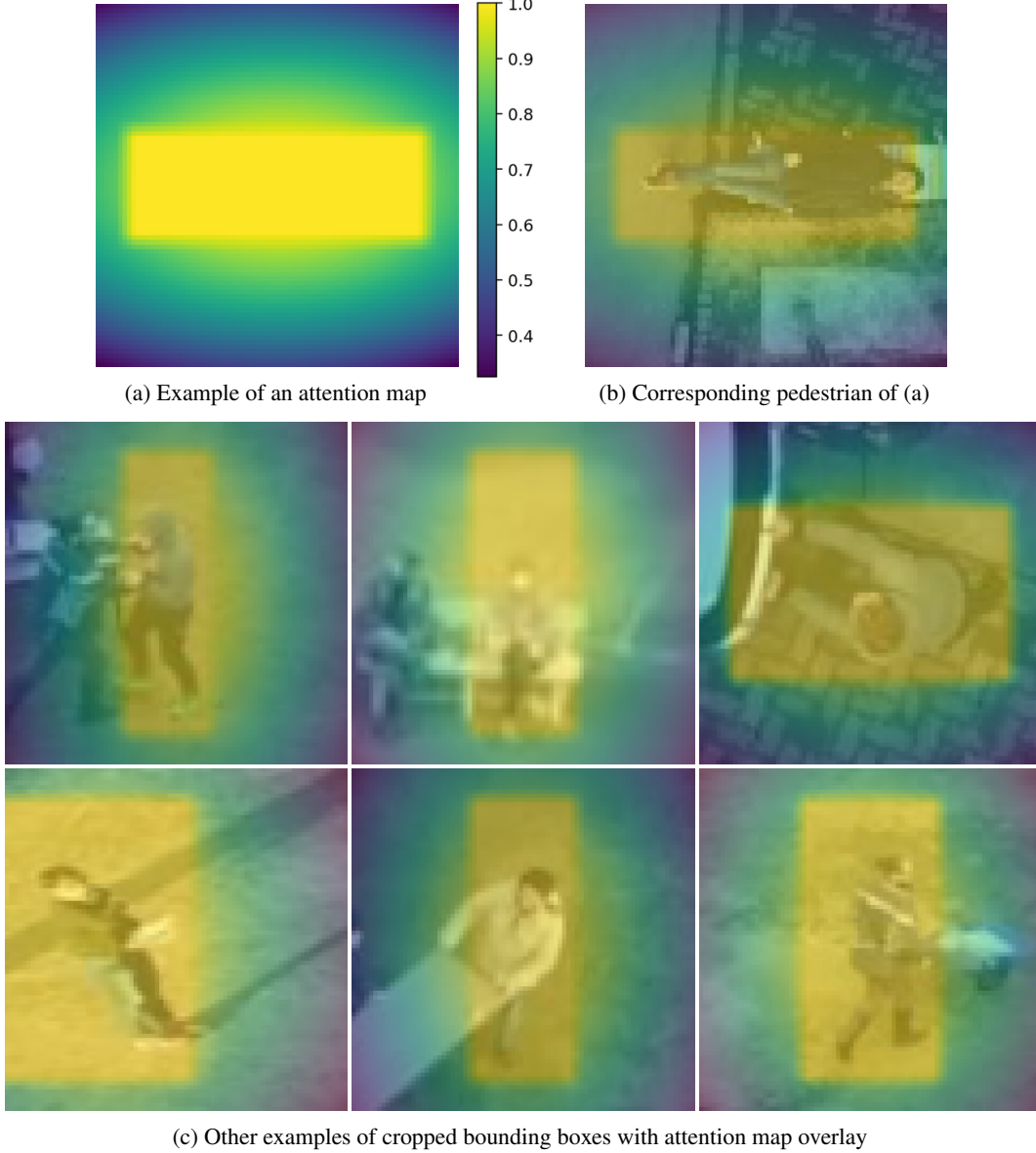


Figure 5: Attention maps are generated to denote which portion of pixels is more significant for the widened bounding boxes. The yellow rectangular shape in each example can be regarded as the original bounding box. A standalone example of an attention map is shown in (a), with the corresponding cropped image shown in (b). More examples of attention maps are shown in (c), which showcase instances that a widened bounding box will add valuable contextual information to the neural networks.

accounts for the multi-activities nature of the dataset. Each pedestrian can be executing a *primary* and a *secondary* action simultaneously. For example, a pedestrian can be *walking* while *pushing* something, or *sitting* while *reading* a book. Let $\bar{\mathbf{p}}_{t,p}^i, \bar{\mathbf{p}}_{t,s}^i$ for $i \in \{1, \dots, N_t\}$ be the corresponding one-hot-encoded ground truth of *primary* and *secondary* activities, where N_t is the number of bounding box at frame t . We will match our predictions using the closest bounding box distance, which gives us the prediction vector $\mathbf{p}_{t,p}^i$ and $\mathbf{p}_{t,s}^i$ for $i \in \{1, \dots, N_t\}$. We can now express the loss function as

$$\mathcal{L}_{ps} = -\frac{1}{T} \sum_{t=1}^T \left(\frac{1}{N_t \cdot N_p} \sum_{i=1}^{N_t} \bar{\mathbf{p}}_{t,p}^i \log \mathbf{p}_{t,p}^i - \lambda_w \frac{1}{N_t \cdot N_s} \sum_{i=1}^{N_t} \bar{\mathbf{p}}_{t,s}^i \log \mathbf{p}_{t,s}^i \right) \quad (6)$$

where T is the total number of frames, N_p , N_s are the number of labels for primary and secondary actions, and λ_w is a weight factor that allows us to balance the two activities differently. In practice, we set $\lambda_w = 0.5$ to focus more on the *primary* action.

4 Experimental Results

In this section, numerical results are reported on pedestrian detection and multi-action recognition tasks, comparing multiple baselines. We also provide empirical results on the deployment of our networks on an embedded device. In particular, the pipeline architecture is deployed on live UAVs to test its field performance and transmission speed. The performance and practicality of the system are evaluated in this section. We used an IoU of 0.5 as the threshold for the following results.

4.1 Dataset

We evaluate our architecture on the *Okutama-Action* dataset (Barekatin, Martí, Shih et al. 2017). It is a publicly available multi-pedestrian drone dataset that contains labels at each frame that describe the pedestrian’s current activities. Deploying a reliable drone-based response system requires recognising the pedestrians’ active state to detect their distress levels. Other aerial surveying datasets exist but do not contain activity labels. The dataset is a high-resolution video dataset captured by UAVs with varying camera angles and altitudes. The dataset consists of 77K fully-annotated frames, where the video sequences are in 4K resolution and 30FPS. Multiple pedestrians exist in a given frame, with labels describing the pedestrians’ current activities. The frames contain varying altitudes, ranging from about 10 to 45 meters, and varying camera angles from 45 degrees to 90 degrees (bird eyes view). The current dataset consists of a labelled bounding box around each person and one or more person’s actions. For example, a person can perform one *primary* action, such as standing or walking, and one *secondary* action, such as carrying or pulling.

4.2 Baselines Models

The following baselines are considered for comparing model performance in our drone dataset.

Models for *multi-activities prediction* we evaluate against (i) SSD RGB (W. Liu, Anguelov, Erhan et al. 2016): pre-trained on ImageNet and fine-tuned to predict individual actions based on fixed-sized images of individual pedestrians; (ii) SSD Optical Flow (Barekatin, Martí, Shih et al. 2017): a variant of the previous baseline that uses motion cues from the optical flow stream; (iii) SSD-MobileNetV2 (Sandler, Howard, Zhu et al. 2018): similar to SSD RGB baseline, but instead MobileNet is used as the feature extractor as a light-weight variant; (iv) Inception-SSD (W. Chen, Qiao and Li 2020): similar to the previous baseline, but instead Inception block is added as an extra layer in the SSD before the prediction; (v) YOLOv3 (Redmon and Farhadi 2018): pre-trained and fine-tuned to the target drone dataset, with an additional LSTM block at the end; (vi) RAER (Ibrahim and Mori 2018): a hierarchical autoencoder-based model that combines scene information with individual action. We follow the main proposed architecture of 4 relational layers and focus on the whole scene.

Models for *pedestrian detection* we evaluate against (i) ReInspect (Stewart, Andriluka and Ng 2016): a joint multi-person detection designed for crowded scene; (ii) ReInspect-rezoom (Stewart, Andriluka and Ng 2016): similar to the last baseline, but with an additional re-zooming layer that transforms features into a scale-invariant representation; (iii) Faster-RCNN (Ren, He, Girshick et al. 2015): a widely adopted region proposal model; (iv) SSD (Szegedy, Vanhoucke, Ioffe et al. 2016): similar to the model that we evaluate in activities prediction, but focus only on proposing bounding boxes; (v) YOLOv3 (W. Liu, Anguelov, Erhan et al. 2016): similarly focuses on bounding boxes proposal.

4.3 Implementation Details

All of our models are trained using the same optimisation and backpropagation scheme. We use the Adam stochastic gradient descent optimiser, with an initial learning rate set to 10^{-4} and fixed hyperparameters to $\beta_1 = 0.9$, $\beta_2 = 0.999$, $\epsilon = 10^{-8}$. We begin by training the pedestrian detection component of each network, which involves using the given ground truth box coordinates to propose bounding boxes. After a fixed number of epochs, we jointly train the temporal components. Gradients are allowed to pass through the previous part, which facilitates each component to compensate for the other in an end-to-end setting.

Method	mAP (%) (primary / secondary)	Inf. time (sec)
Ours	24.2 / 13.6	1.43 ± 0.21
Ours (w/o att.)	22.5 / 12.3	1.41 ± 0.23
SSD RGB (W. Liu, Anguelov, Erhan et al. 2016)	18.8 / 7.41	2.02 ± 0.39
SSD Optical Flow (W. Liu, Anguelov, Erhan et al. 2016)	6.47 / 2.21	1.91 ± 0.37
SSD-MobileNetV2 (Sandler, Howard, Zhu et al. 2018)	17.2 / 7.10	1.88 ± 0.22
Inception-SSD (W. Chen, Qiao and Li 2020)	19.6 / 9.51	2.02 ± 0.39
YOLOv3-LSTM (Redmon and Farhadi 2018)	20.2 / 9.96	2.21 ± 0.65
RAER (Ibrahim and Mori 2018)	21.5 / 10.56	3.16 ± 0.64

Table 1: Multi action recognition performed on the embedded system TX2. Inference time is in ($\mu \pm 2\sigma$) seconds.

4.4 Model Deployment on Embedded-UAV

The overall drone and the onboard system are illustrated in Fig. 6. The pipeline architecture is first trained on an external server to speed up training time. The coding environment is developed on top of the Python Deep-Learning *PyTorch* library. Then, the trained model is converted to a Caffe model that can be run natively without the Python runtime environment. We packaged the model as an onboard application and deployed it to the NVIDIA Jetson TX2. The NVIDIA Jetson TX2 is an embedded AI computing device that enables edge computing with an NVIDIA Pascal GPU with 8 GB RAM. The Jetson TX2 then acted as the onboard computer and attached to the DJI Matrice 100 (Fig. 6a). The TX2 is mounted on the Auvideo J120 carrier board and connects to the UAV using a USB to TTL/UART connection. We attached a Logitech C920 camera (Fig. 6b) to capture video footage, and an LTE dongle to the Jetson TX2 to communicate information back to the user. The onboard battery for the UAV is a DJI TB48D battery with 130 watt-hours, acting as the power source to the onboard computer through a voltage regulator (Fig. 6c) to maintain a constant voltage for the embedded board. The USB camera capture footage and streams it to the Caffe model to perform inference. The total payload of the entire onboard setup during the field test (Fig. 1) is at around 0.57 kg.

During deployment, an image frame is first fetched from the video feed, resized, and sent to the Caffe model. The frame extraction procedure is performed using the OpenCV C++ library, typically taking < 5 milliseconds. Then, the frame is passed to the POINet, followed by the ActivityNet for the whole inference procedure. The embedded processing device typically takes around 2-3 seconds to process each frame and transmit the corresponding information. Depending on the number of detected pedestrians, the drone will then uses around 100 – 500 bytes of network bandwidth to send the information back to the remote operator.

4.5 Multi-Pedestrian Multi-activities Recognition

In table 1, we report the mean average precision (mAP) and inference time on the NVIDIA Jetson TX2 embedded on UAV during deployment. We report accuracies separately for the primary and secondary actions by the pedestrians. We take the top two predicted outputs as primary and secondary actions for models that do not predict multiple actions. We also report a variant of our model without the additional attention map (section 3.3.1) to evaluate its effectiveness. Inference time performed on the embedded device reports the mean and the 95% quantile over 30 runs in seconds.

Overall, our model achieves state-of-the-art performance for both *primary* and *secondary* actions recognition even without the ground truth locations of the individuals. The comparison to SSD variants, which propose pedestrians’ action based purely on captured frames, indicates that having a temporal joint representation shared across multiple tasks helps us improve accuracy. YOLOv3-LSTM and RAER perhaps are the main competitor as they utilise temporal information across frames. Of the two, RAER performs better as it utilises a hierarchical structure and scene information. However, the architecture also imposes more overhead in inference time, which is essential in a real-time UAV application with limited processing power. In fact, our model requires the lowest inference time as our model requires fewer parameters and uses operations that cut down runtime. Our attention map approach also helps to improve performance, which is likely due to the extra information around the boundary that would otherwise be cropped (Fig. 5). Such an approach also helps to maintain the aspect ratio of the input to our temporal component. Our algorithmic attention map will likely be less performant than a learning approach; however, it requires little to no overhead to generate, which is essential in time-sensitive applications. Fig. 1 and Fig. 4 are results from our actual running model.

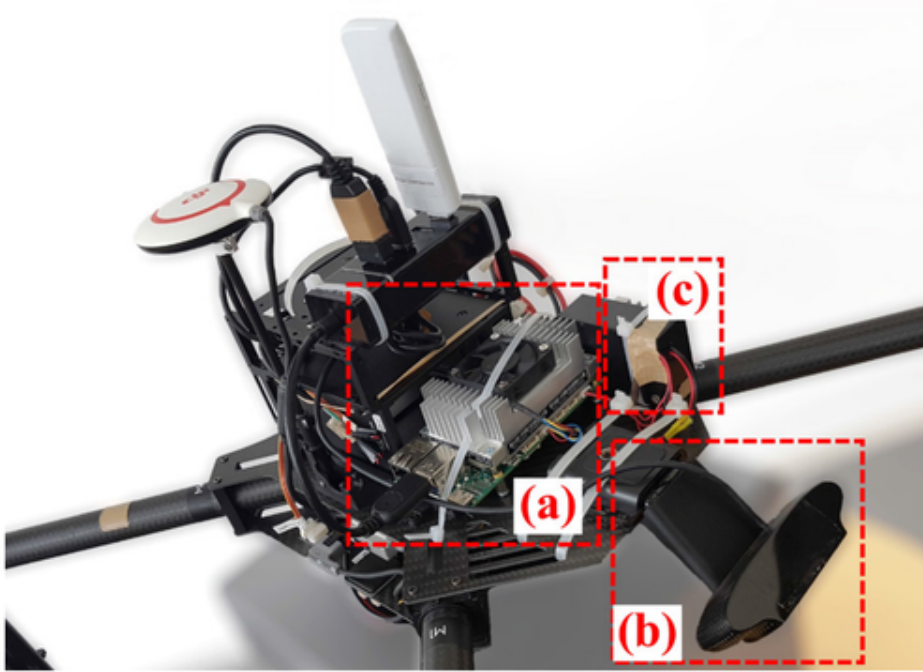


Figure 6: DJI Matrice 100 drone with an embedded TX2 device used for the field test and inference benchmark. (a) NVIDIA Jetson TX2, (b) Logitech C920 camera, (c) voltage regulator.

Method	mAP (%)	Inf. time (sec)
POINet (ours)	84.5	1.52 ± 0.16
ReInspect (Stewart, Andriluka and Ng 2016)	79.8	3.41 ± 0.77
ReInspect-rezoom (Stewart, Andriluka and Ng 2016)	81.1	3.50 ± 0.69
Faster-RCNN (Ren, He, Girshick et al. 2015)	68.1	2.98 ± 0.42
SSD (W. Liu, Anguelov, Erhan et al. 2016)	72.3	1.98 ± 0.37
YOLOv3 (Redmon and Farhadi 2018)	77.2	2.38 ± 0.52

Table 2: Results for multi-pedestrian detection from UAVs imagery. Inference time is in ($\mu \pm 2\sigma$) seconds.

4.6 Multi-Pedestrian Detection

In addition to evaluating the overall performance of action recognition, we also conducted a standalone experiment evaluating the performance for POINet to propose bounding boxes from UAV imagery. Our evaluation of pedestrian detection from the UAV dataset (table 2) found that existing box proposal approaches do not work well in sparse scenes with varying camera angles. For example, our leading contender ReInspect works well in a dense proposal of a crowded scene as shown in (Stewart, Andriluka and Ng 2016). However, it does not perform well in UAV imagery, mainly when the objects of interest are sparsely spaced, which introduces more false positives in the model output. The addition of an invariant layer in ReInspect-rezoom helps enhance the performance as it scales better with smaller objects. However, both models require quite a significant runtime overhead due to the need to make joint predictions in a sequential manner. It should be noted that SSD, YOLO and RCNN models are built to propose bounding boxes for various objects. That is, they are capable of proposing bounding boxes with more than one class as they are designed for dense proposals of day-to-day objects. However, for a domain-specific application where we are only interested in search and rescue in a sparse environment (e.g. in a wide open field), these model assumptions do not seem to perform well. Therefore, using them solely for pedestrian detection seems to limit their predictability in our UAV application. By exploiting the domain specificity, our proposed POINet achieves higher precision with less computational overhead.

5 Conclusions

We have proposed a novel approach for real-time UAV applications by exploiting domain knowledge. Our model is designed to excel in detecting pedestrians regardless of their orientation from UAV's perspective. It is lightweight and combines traditional computer vision techniques to acquire the anchor points of boxes: harnessing the rich representation power of the deep learning model for robust drone operations.

The constraints of performing inference directly onboard can severely limit the potential model complexity. In our deployment, when our framework detects pedestrians and decides to report their status, it will transmit a message of 100–500 bytes to its operator (depending on the number of detected pedestrians). Compared to streaming videos to a remote server for inference, it will take a continuous stream of images, each with about 200 kB. Constructing a jointed detection and recognition model with constraints on output message size ensures model deployment's practicality in a distributed and reliable manner.

5.1 Limitations

Our model's limitations include only focusing on detecting pedestrians, as opposed to general objects like other approaches. Moreover, it is likely that our bounding box proposal mechanism would not perform well in cluttered scenarios, which is uncommon for disaster response in a remote area. For future work, for a more UAV domain-specific approach, we can utilise altitude or velocity information from drone sensors as model features to provide more details during inference. This approach might allow the model to account for the problematic scenarios and uncertainty issues in UAV imagery.

5.2 Potential negative societal impact

While the usage of UAVs in rural environments for disaster responses has been proven effective, the emergence of ubiquitous consumer UAV hardware has raised concerns. The learning of a pedestrian tracking and reasoning model in autonomous UAVs can have potential negative impacts on privacy issues, for example, deployments of aerial surveillance in cities. Potential negative impacts can be minimised by imposing governmental policies and social-wise regulations. In UAV-based anomaly detection, we can impose restrictions that the extracted pedestrians' information is only processed directly onboard. If the UAV detects anomalies that require further actions by human operators, UAVs will only then transmit anonymised data to operators.

References

- Abdelkader, Mohamed, Mohammad Shaqura, Christian G. Claudel and Wail Gueaieb (2013). 'A UAV Based System for Real Time Flash Flood Monitoring in Desert Environments Using Lagrangian Microsensors'. In: *2013 International Conference on Unmanned Aircraft Systems (ICUAS)*. 2013 International Conference on Unmanned Aircraft Systems (ICUAS). DOI: 10.1109/icuas.2013.6564670.
- Aljehani, Maher and Masahiro Inoue (2016). 'Multi-UAV Tracking and Scanning Systems in M2M Communication for Disaster Response'. In: *2016 IEEE 5th Glob. Conf. Consum. Electron. IEEE*. DOI: 10.1109/gcce.2016.7800524.
- Amato, Giuseppe, Luca Ciampi, Fabrizio Falchi and Claudio Gennaro (2019). 'Counting Vehicles with Deep Learning in Onboard Uav Imagery'. In: *2019 IEEE Symp. Comput. Commun. ISCC*. IEEE. DOI: 10.1109/ISCC47284.2019.8969620.
- Andrew, William, Colin Greatwood and Tilo Burghardt (2019). 'Aerial Animal Biometrics: Individual Friesian Cattle Recovery and Visual Identification via an Autonomous Uav with Onboard Deep Inference'. In: *2019 IEEERSJ Int. Conf. Intell. Robots Syst. IROS*. IEEE. DOI: 10.1109/IROS40897.2019.8968555.
- Bagautdinov, Timur, Alexandre Alahi, François Fleuret, Pascal Fua and Silvio Savarese (2017). 'Social Scene Understanding: End-to-end Multi-Person Action Localization and Collective Activity Recognition'. In: *Proceedings of the IEEE Conference on Computer Vision and Pattern Recognition*. DOI: 10.1109/CVPR.2017.365.
- Bai, Yong, Wencai Du, Zhengxin Ma, Chong Shen, Youling Zhou and Baodan Chen (2010). 'Emergency Communication System by Heterogeneous Wireless Networking'. In: *2010 IEEE Int. Conf. Wirel. Commun. Netw. Inf. Secur.* IEEE.
- Barekatain, Mohammadamin, Miquel Martí, Hsueh-Fu Shih, Samuel Murray, Kotaro Nakayama, Yutaka Matsuo and Helmut Prendinger (2017). 'Okutama-Action: An Aerial View Video Dataset for Concurrent Human Action Detection'. In: *Proceedings of the IEEE Conference on Computer Vision and Pattern Recognition Workshops*. DOI: 10.1109/CVPRW.2017.267.

- Bejiga, Mesay, Abdallah Zeggada, Abdelhamid Nouffidj and Farid Melgani (2017). ‘A Convolutional Neural Network Approach for Assisting Avalanche Search and Rescue Operations with Uav Imagery’. In: *Remote Sens.* 9.2, p. 100. DOI: 10.3390/rs9020100.
- Bishop, Christopher M (2006). *Pattern Recognition and Machine Learning*. springer.
- Borji, Ali and Laurent Itti (2012). ‘State-of-the-Art in Visual Attention Modeling’. In: *IEEE Transactions on Pattern Analysis and Machine Intelligence* 35.1, pp. 185–207. DOI: 10.1109/tpami.2012.89.
- Chen, Wanpei, Yanting Qiao and Yujie Li (2020). ‘Inception-SSD: An Improved Single Shot Detector for Vehicle Detection’. In: *J. Ambient Intell. Humaniz. Comput.*, pp. 1–7.
- Chen, Yu Ming, Liang Dong and Jun-Seok Oh (2007). ‘Real-Time Video Relay for Uav Traffic Surveillance Systems through Available Communication Networks’. In: *2007 IEEE Wirel. Commun. Netw. Conf. IEEE*. DOI: 10.1109/wcnc.2007.485.
- Chu, Xiao, Wei Yang, Wanli Ouyang, Cheng Ma, Alan L Yuille and Xiaogang Wang (2017). ‘Multi-Context Attention for Human Pose Estimation’. In: *Proceedings of the IEEE Conference on Computer Vision and Pattern Recognition*.
- Cooijmans, Tim, Nicolas Ballas, César Laurent, Çağlar Gülçehre and Aaron C. Courville (2017). ‘Recurrent Batch Normalization’. In: *5th Int. Conf. Learn. Represent. ICLR 2017 Toulon Fr. April 24-26 2017 Conf. Track Proc.*
- Dike, Happiness Ugochi, Qingtian Wu, Yimin Zhou and Gong Liang (2018). ‘Unmanned Aerial Vehicle (UAV) Based Running Person Detection from a Real-Time Moving Camera’. In: *2018 IEEE International Conference on Robotics and Biomimetics (ROBIO)*. IEEE. DOI: 10/gnbp6s.
- Douklias, Athanasios, Lazaros Karagiannidis, Fay Misichroni and Angelos Amditis (2022). ‘Design and Implementation of a UAV-Based Airborne Computing Platform for Computer Vision and Machine Learning Applications’. In: *Sensors* 22.5, p. 2049. DOI: 10.3390/s22052049.
- Häger, Gustav, Goutam Bhat, Martin Danelljan, Fahad Shahbaz Khan, Michael Felsberg, Piotr Rudl and Patrick Doherty (2016). ‘Combining Visual Tracking and Person Detection for Long Term Tracking on a Uav’. In: *International Symposium on Visual Computing*. Springer.
- Hildmann, Hanno and Ernő Kovacs (2019). ‘Using Unmanned Aerial Vehicles (UAVs) as Mobile Sensing Platforms (MSPs) for Disaster Response, Civil Security and Public Safety’. In: *Drones* 3.3, p. 59. DOI: 10.3390/drones3030059.
- Hong, Seunghoon, Junhyuk Oh, Honglak Lee and Bohyung Han (2016). ‘Learning Transferrable Knowledge for Semantic Segmentation with Deep Convolutional Neural Network’. In: *Proceedings of the IEEE Conference on Computer Vision and Pattern Recognition*.
- Hu, Hansel, Tin Lai and Farnaz Farid (2022). ‘Feasibility Study of Constructing a Screening Tool for Adolescent Diabetes Detection Applying Machine Learning Methods’. In: *Applications of Body Worn Sensors and Wearables*, Special Issue of *Sensors* 22.16, p. 6155. ISSN: 1424-8220. DOI: 10.3390/s22166155. URL: <https://www.mdpi.com/1424-8220/22/16/6155>.
- Huang, Kai, Ximeng Liu, Shaojing Fu, Deke Guo and Ming Xu (2019). ‘A Lightweight Privacy-Preserving CNN Feature Extraction Framework for Mobile Sensing’. In: *IEEE Transactions on Dependable and Secure Computing*.
- Hulens, Dries, Toon Goedemé and Jon Verbeke (2015). ‘How to Choose the Best Embedded Processing Platform for On-Board UAV Image Processing?’ In: *Proceedings VISAPP 2015*, pp. 1–10.
- Ibrahim, Mostafa S and Greg Mori (2018). ‘Hierarchical Relational Networks for Group Activity Recognition and Retrieval’. In: *Proceedings of the European Conference on Computer Vision (ECCV)*. DOI: 10.1007/978-3-030-01219-9_44.
- Ji, Shuiwang, Wei Xu, Ming Yang and Kai Yu (2013). ‘3D Convolutional Neural Networks for Human Action Recognition’. In: *IEEE transactions on pattern analysis and machine intelligence* 35.1, pp. 221–231.
- Al-Kaff, Abdulla, David Martin, Fernando Garcia, Arturo de la Escalera and Jose Maria Armingol (2018). ‘Survey of Computer Vision Algorithms and Applications for Unmanned Aerial Vehicles’. In: *Expert Systems With Applications* 92, pp. 447–463. DOI: 10.1016/j.eswa.2017.09.033.
- Kakaletsis, Efstratios, Charalampos Symeonidis, Maria Tzelepi, Ioannis Mademlis, Anastasios Tefas, Nikos Nikolaidis and Ioannis Pitas (2021). ‘Computer Vision for Autonomous UAV Flight Safety: An Overview and a Vision-Based Safe Landing Pipeline Example’. In: *ACM Comput. Surv. CSUR* 54.9, pp. 1–37. DOI: 10.1145/3472288.
- Karaca, Yunus, Mustafa Cicek, Ozgur Tatli, Aynur Sahin, Sinan Pasli, Muhammed Fatih Beser and Suleyman Turedi (2018). ‘The Potential Use of Unmanned Aircraft Systems (Drones) in Mountain Search and Rescue Operations’. In: *American Journal of Emergency Medicine* 36.4, pp. 583–588. DOI: 10.1016/j.ajem.2017.09.025.
- Kraft, Marek, Mateusz Piechocki, Bartosz Ptak and Krzysztof Walas (2021). ‘Autonomous, Onboard Vision-Based Trash and Litter Detection in Low Altitude Aerial Images Collected by an Unmanned Aerial Vehicle’. In: *Remote Sensing* 13.5, p. 965. DOI: 10/gjkt3z.
- Lai, Tin (2022). ‘A Review on Visual-SLAM: Advancements from Geometric Modelling to Learning-Based Semantic Scene Understanding Using Multi-Modal Sensor Fusion’. In: *Sensors* 22.19, p. 7265.
- Lai, Tin and Fabio Ramos (2022). ‘Adaptively Exploits Local Structure with Generalised Multi-Trees Motion Planning’. In: *IEEE Robotics and Automation Letters (RA-L)* 7.2, pp. 1111–1117. DOI: 10.1109/LRA.2021.3132985.

- Lai, Tin, Weiming Zhi, Tucker Hermans and Fabio Ramos (2022). ‘L4KDE: Learning for KinoDynamic Tree Expansion’. In: *Computing Research Repository (CoRR)*.
- Liu, Wei, Dragomir Anguelov, Dumitru Erhan, Christian Szegedy, Scott Reed, Cheng-Yang Fu and Alexander C Berg (2016). ‘Ssd: Single Shot Multibox Detector’. In: *Eur. Conf. Comput. Vis.* Springer. DOI: 10.1007/978-3-319-46448-0_2.
- Merino, Luis, Fernando Caballero, J Ramiro Martínez-de Dios, Joaquín Ferruz and Anibal Ollero (2006). ‘A Cooperative Perception System for Multiple UAVs: Application to Automatic Detection of Forest Fires’. In: *Journal of Field Robotics* 23.3-4, pp. 165–184.
- Neubeck, Alexander and Luc Van Gool (2006). ‘Efficient Non-Maximum Suppression’. In: *18th Int. Conf. Pattern Recognit. ICPR06*. IEEE. DOI: 10.1109/icpr.2006.479.
- Ouyang, Wanli and Xiaogang Wang (2013). ‘Joint Deep Learning for Pedestrian Detection’. In: *Proceedings of the IEEE International Conference on Computer Vision*. DOI: 10.1109/ICCV.2013.257.
- Ramanathan, Vignesh, Jonathan Huang, Sami Abu-El-Haija, Alexander Gorban, Kevin Murphy and Li Fei-Fei (2016). ‘Detecting Events and Key Actors in Multi-Person Videos’. In: *Proceedings of the IEEE Conference on Computer Vision and Pattern Recognition*. DOI: 10.1109/CVPR.2016.332.
- Redmon, Joseph, Santosh Divvala, Ross Girshick and Ali Farhadi (2016). ‘You Only Look Once: Unified, Real-Time Object Detection’. In: *The IEEE Conference on Computer Vision and Pattern Recognition (CVPR)*. DOI: 10.1109/cvpr.2016.91.
- Redmon, Joseph and Ali Farhadi (2018). *Yolov3: An Incremental Improvement*. arXiv: 1804.02767.
- Ren, Shaoqing, Kaiming He, Ross Girshick and Jian Sun (2015). ‘Faster R-cnn: Towards Real-Time Object Detection with Region Proposal Networks’. In: *Advances in neural information processing systems* 28, pp. 91–99.
- Sahingoz, Ozgur Koray (2013). ‘Mobile Networking with UAVs: Opportunities and Challenges’. In: *2013 International Conference on Unmanned Aircraft Systems (ICUAS)*. IEEE.
- Sambolek, Sasa and Marina Ivacic-Kos (2020). ‘Person Detection in Drone Imagery’. In: *2020 5th International Conference on Smart and Sustainable Technologies (SpliTech)*. IEEE. DOI: 10/gnbp6v.
- Sandler, Mark, Andrew Howard, Menglong Zhu, Andrey Zhmoginov and Liang-Chieh Chen (2018). ‘Mobilenetv2: Inverted Residuals and Linear Bottlenecks’. In: *Proceedings of the IEEE Conference on Computer Vision and Pattern Recognition*. DOI: 10.1109/CVPR.2018.00474.
- Schulte, S., F. Hillen and T. Prinz (2017). ‘Analysis of Combined Uav-Based Rgb and Thermal Remote Sensing Data: A New Approach to Crowd Monitoring’. In: *ISPRS - International Archives of the Photogrammetry, Remote Sensing and Spatial Information Sciences XLII-2/W6*, pp. 347–354. ISSN: 2194-9034. DOI: 10.5194/isprs-archives-xlii-2-w6-347-2017. URL: <https://www.int-arch-photogramm-remote-sens-spatial-inf-sci.net/XLII-2-W6/347/2017/> (visited on 18/08/2020).
- Sozykin, Konstantin, Stanislav Protasov, Adil Khan, Rasheed Hussain and Jooyoung Lee (2018). ‘Multi-Label Class-Imbalanced Action Recognition in Hockey Videos via 3D Convolutional Neural Networks’. In: *2018 19th IEEE/ACIS International Conference on Software Engineering, Artificial Intelligence, Networking and Parallel/Distributed Computing (SNPD)*. IEEE. DOI: 10/gnbp6t.
- Stewart, Russell, Mykhaylo Andriluka and Andrew Y Ng (2016). ‘End-to-End People Detection in Crowded Scenes’. In: *Proceedings of the IEEE Conference on Computer Vision and Pattern Recognition*. DOI: 10.1109/CVPR.2016.255.
- Szegedy, Christian, Vincent Vanhoucke, Sergey Ioffe, Jon Shlens and Zbigniew Wojna (2016). ‘Rethinking the Inception Architecture for Computer Vision’. In: *Proceedings of the IEEE Conference on Computer Vision and Pattern Recognition*. DOI: 10.1109/CVPR.2016.308.
- Tian, Yonglong, Ping Luo, Xiaogang Wang and Xiaoou Tang (2015). ‘Deep Learning Strong Parts for Pedestrian Detection’. In: *Proceedings of the IEEE International Conference on Computer Vision*. DOI: 10.1109/ICCV.2015.221.
- Vega, Augusto, Chung-Ching Lin, Karthik Swaminathan, Alper Buyuktosunoglu, Sharathchandra Pankanti and Pradip Bose (2015). ‘Resilient, UAV-embedded Real-Time Computing’. In: *2015 33rd IEEE International Conference on Computer Design (ICCD)*. IEEE.
- Wang, Chu and Kaleem Siddiqi (2016). ‘Differential Geometry Boosts Convolutional Neural Networks for Object Detection’. In: *Proceedings of the IEEE Conference on Computer Vision and Pattern Recognition Workshops*.
- Wang, Xiaoliang, Peng Cheng, Xinchuan Liu and Benedict Uzochukwu (2018). ‘Fast and Accurate, Convolutional Neural Network Based Approach for Object Detection from UAV’. In: *IECON 2018-44th Annual Conference of the IEEE Industrial Electronics Society*. IEEE. DOI: 10/gnbp6q.
- Wang, Xiaoyu, Tony X Han and Shuicheng Yan (2009). ‘An HOG-LBP Human Detector with Partial Occlusion Handling’. In: *2009 IEEE 12th Int. Conf. Comput. Vis.* IEEE. DOI: 10.1109/ICCV.2009.5459207.
- Wang, Xipei, Haoyu Zhang, Yuanbo Zhang, Meng Wang, Jiarui Song, Tin Lai and Matloob Khushi (2022). ‘Learning Non-Stationary Time-Series with Dynamic Pattern Extractions’. In: *IEEE Transactions on Artificial Intelligence (TAI)* 3.5, pp. 778–787. DOI: 10.1109/TAI.2021.3130529.

- Xu, Huijuan, Abir Das and Kate Saenko (2017). ‘R-C3d: Region Convolutional 3d Network for Temporal Activity Detection’. In: *Proceedings of the IEEE International Conference on Computer Vision*.
- Xu, Xiaoting, Tin Lai, Sayka Jahan, Farnaz Farid and Abubakar Bello (2022). ‘A Machine Learning Predictive Model to Detect Water Quality and Pollution’. In: *Future Internet* 14.11, p. 324.
- Xu, Zhaozhuo, Xin Xu, Lei Wang, Rui Yang and Fangling Pu (2017). ‘Deformable Convnet with Aspect Ratio Constrained Nms for Object Detection in Remote Sensing Imagery’. In: *Remote Sens.* 9.12, p. 1312. DOI: 10.3390/rs9121312.
- Yang, Jianxiu, Xuemei Xie and Wenzhe Yang (2019). ‘Effective Contexts for UAV Vehicle Detection’. In: *IEEE access : practical innovations, open solutions* 7, pp. 85042–85054.
- Zhang, Ruiqian, Zhenfeng Shao, Xiao Huang, Jiaming Wang and Deren Li (2020). ‘Object Detection in UAV Images via Global Density Fused Convolutional Network’. In: *Remote Sensing* 12.19, p. 3140. DOI: 10/gh2j82.
- Zheng, Heliang, Jianlong Fu, Tao Mei and Jiebo Luo (2017). ‘Learning Multi-Attention Convolutional Neural Network for Fine-Grained Image Recognition’. In: *Proceedings of the IEEE International Conference on Computer Vision*. DOI: 10.1109/ICCV.2017.557.
- Zheng, Liang, Yali Zhao, Shengjin Wang, Jingdong Wang and Qi Tian (2016). *Good Practice in CNN Feature Transfer*. arXiv: 1604.00133.